

Blended Coatings from Polyaniline (PANI) and Chemically Doped Sodium Docecyl Benzene Sulphonate (SDBS)/SiO₂ Nanocomposites: Influence on Corrosion Protection of Mild Steel

N.Dhana Raj

Central Institute of Plastics Engineering and Technology (CIPET), Chennai, Tamil nadu.

Smita Mohanty (✉ drsmitamohanty@gmail.com)

CIPET: Central Institute of Plastics Engineering and Technology <https://orcid.org/0000-0002-3697-3272>

Sanjay Nayak (Self-nomination)

Central Institute of Plastics Engineering and Technology (CIPET), Chennai, Tamil nadu.

Research Article

Keywords: PANI, Coating, Corrosion, nanocomposite

Posted Date: April 21st, 2021

DOI: <https://doi.org/10.21203/rs.3.rs-442933/v1>

License: © ⓘ This work is licensed under a Creative Commons Attribution 4.0 International License.

[Read Full License](#)

Blended Coatings from Polyaniline (PANI) and Chemically doped Sodium docecyl benzene sulphonate (SDBS)/SiO₂ Nanocomposites: Influence on Corrosion Protection of Mild Steel

N.Dhana Raj¹, SmitaMohanty², S K Nayak^{1,2*}

Central Institute of Plastics Engineering and Technology (CIPET), Chennai, Tamil nadu.

School for Advanced in Polymers (SARP) Laboratory for Advanced Research in Polymeric Materials (LARPM), CIPET Bhubaneswar, Odisha.

E Mail:drsknayak@yahoo.com

ABSTRACT

In this work, investigation on corrosion protection performance of chemically synthesized polyaniline (PANI) / SiO₂nanocomposite coatings has been carried out on Mild Steel (MS). Sodium docecyl benzene sulphonate (SDBS) doped conducting PANI / SiO₂at different ratios was synthesized by employing in -situ polymerization technique. The developed coatings were characterized using Fourier transform infrared spectroscopy (FTIR), Thermo gravimetric analysis (TGA), Transmission electron microscopy (TEM), Contact angle, Atomic force microscopy (AFM) and corrosion analysis. The FTIR analysis indicates the strong interaction between PANI and SiO₂ nanoparticles. The contact angle study reveals the hydrophilicity character of the nanocomposite coatings with a water contact angle of 74.9°. Corrosion resistanceof uncoated mild steel and the coated sample in 3.5 % NaCl aqueous solution has been evaluated using weight loss methods. Additionally the Electrochemical Impedance Spectroscopy (EIS) studies have been also conducted to evaluate the coorision protection characteristics of the coatings. PANI containing SiO₂ (PSC III) coating showed excellent resistance after immersion in 3.5 % NaCl solution for 1 month time period.

Keywords: PANI, Coating, Corrosion,nanocomposite

INTRODUCTION:

Corrosion process which involves gradual destruction of materials exposed to environmental conditions through chemical or electrochemical reactions has been a primary concern globally. Around 3% of the global gross domestic product (GDP) annually is effected by the corrosion process[1-2].Corrosion protection employing polymeric coatings have generated considerable research interests in the recent years. Conducting polymers such as polypyrrole, polythiophene, polyaniline, polyacetylene etc. have been reported to be widely employed as coatings over the metal substrates to these substrates against corrosion [3-4]. Amongst the various conducting polymers, polyaniline (PANI) based systems have been reported to demonstrate improved corrosion protection properties as compared with the other polymers [3].

PANI known for its conducting properties [5] has good stability, high electrical conductivity [6] in addition to energy storage and electrochemical properties. PANI has been employed for multitude of applications like sensors, super capacitors, electrochromic display, fuel cells rechargeable organic batteries, drug delivery as well as in corrosion protection coatings. However, the major impediments of PANI includes limitations in processability predominantly due to its insolubility in majority of common solvents; brittle structure which prevents its wider applicability. These problems can be largely averted by changing the oxidation state of PANI, incorporation of dopants or preparing blends/composites of PANI with other polymers and reinforcing it with nanofillers[7].

Conducting polymer composites of PANI reinforced with nano fillers have been known to show its potentiality for corrosion protection. Encapsulated metal oxide based particles within the shell of PANI have bestowed improved physico-mechanical and chemical properties while retaining the conducting properties with synergism between the matrix polymer and the

inorganic particles [8-9]. Several inorganic/organic particles like SiO₂, TiO₂, Graphene, Fe₃O₄, ZnO, ZnMoO₄ etc have been reinforced within PANI employing emulsion polymerisation technique to achieve desired attributes [10].

Among various inorganic particles, SiO₂ nanoparticles having a porous structure can be suitably modified for its potential application in corrosion protection coatings [11]. Al-Dulaimi A et al have reported single step insitu method of synthesising PANI/SiO₂ composite having improved corrosion protection characteristics in corrosive solvents [12]. Similar several reports pertaining to the anti-corrosive paints of PANI/SiO₂ have been reported by several workers have been reported [13-20].

In the current investigation PANI/SiO₂ nanocomposite coatings has been prepared using single step-in-situ-polymerisation technique. Sodium dodecyl benzene sulphonic acid (SDBS) was used as a dopant owing to its improved solubility. An in-depth study on the morphology of the synthesised nanocomposite coatings was carried out employing Fourier Transform Infrared spectroscopy (FTIR), Transmission electron microscopy, X-ray diffraction (XRD) and atomic force microscopy. The corrosion study was investigated through weigh loss method and the electrochemical impedance spectroscopy and contact angle study of the nanocomposite coatings have been reported.

2. Experimental

2.1 Material

Aniline procured from M/s NICE chemicals Pvt. Ltd, Kochi, Kerala, India and distilled prior to its use and stored at 10⁰ C. SDBS (Sodium Dodecyl Benzene Sulphonate), 1-methyl-2-pyrrolidone (NMP), and APS (ammonium persulphate), were purchased from M/s Himedia India. Nanosilica (175–225 m²/g[BET]) with 90% purity was purchased from M/s Sigma Aldrich USA. Epoxy clear with amine hardener (Finehard 486) was procured from

M/s Fine finish organics Pvt Ltd, Mumbai, India. Xylene, Sodium chloride (NaCl), 1-butanol and double distilled water were used for solution preparation. Stainless steel coupons for corrosion studies were purchased locally from Bhubaneswar, Odisha.

2.2 Synthesis of PANI/ SiO₂Nanocomposite Coatings

PANI/ SiO₂nanocomposite coatings were prepared using chemical oxidative using ammonium persulphate (APS) as the initiator in 1(M) HCl solution. In a four necked round bottom flask, 100 ml solution comprising of 0.2 M Aniline and 0.04 M SDBS was taken to which 0.1 g of nano-SiO₂ was added. Subsequently, 0.2 M APS was added drop wise and the reaction was carried out under nitrogen atmosphere for 3h at 5⁰ C in an ultrasonic bath to ensure complete the polymerization process. Nano-SiO₂:Aniline weight ratio was maintained at 0.10:1(PANI/SiO₂-I). Then, the reaction mixture was kept at equilibrium state for 4 h and the final product obtained was filtered, washed with double distilled water till colorless filtrate was obtained and then dried at 60⁰ C for 24 h in air oven. The aforesaid process was repeated to synthesize nanocomposites at variable weight ratios of Nano-SiO₂:Aniline - 0.15:1(PANI/SiO₂-II) and 0.20:1(PANI/SiO₂-III) respectively.

2.3 Preparation of PANI/ SiO₂composites coating on mild steel

Mild steel panels were coated at variable loadings of PANI/SiO₂(PSC) and neat PANI formulated with epoxy resin to evaluate the corrosion resistance properties of the coatings. Prior to coating the surface of the mild steel panels were subjected to gritting using emery paper followed by washing and cleaning with trichloroethylene and acetone to remove contamination if any on the surface. 6g of solid epoxy resin was dissolved in 4 ml xylene solution to which 1% PANI/SiO₂ solution was added and ultrasonicated for 2 hrs. Then 1g hardener was added and the mixture was further sonicated for 1 hr to obtain the coating formulation. Xylene– butanol mixture at a ratio of 9:3 was added to maintain the viscosity of

coating. Finally the coating formulation was coated onto mild steel substrate of 1 cm² using drop coating method and was dried at 600 °C for 4 h. A coating thickness of 110± 10 μm was maintained in all the formulations.

2.4 Characterization of the PANI and its nanocomposite coatings

After the successful growth of polymer nanocomposite coatings, the microstructural and electrochemical corrosion properties were investigated using various characterization tools. The structural information of polymer nanocomposite coatings was performed using Fourier transform infrared (FTIR) spectroscopy (Thermo Scientific, Nicolet 6700, USA) in the attenuated total reflectance mode from 400-4000 cm⁻¹. The X-ray diffraction pattern of the polymer nanocomposite coatings were examined using Shimadzu X-ray diffractometer with a measuring angle from 5 to 80° and the scan rate was maintained 5°/min. The surface morphology of the polymer nanocomposites was characterized by Transmission electron microscopy (TEM, 1400 JEOL Japan). Samples of ~2 mg was dispersed in 5 ml of ethanol and sonicated for 5 mins to disperse uniformly. A drop dispersed solution was then placed on a copper grid and kept in the oven for complete dry or evaporate the sample. The surface topography and roughness of the coatings were examined using Atomic Force Microscopy (AFM, XE-100). The measurements were performed in non-contact mode at room temperature. The wetting properties of the coated surface was acquired by contact angle measurement (Phoenix SEO Pvt. Ltd, Korea). The thermal stability of the samples was examined by Thermogravimetric analysis (TGA) (M/s TA instruments, USA) at a heating rate of 10°C/min in the temperature range from 30 to 700 °C under nitrogen atmosphere.

2.4.1 Electrochemical Impedance studies (EIS):

The electrochemical characteristics of as-prepared epoxy and PS coatings were tested using an electrochemical workstation in 3.5% NaCl solution. The exposed area of the coating

is 1 cm². The EIS and Tafel are measured in a three-electrode system. The coated substrate was a working electrode, saturated calomel electrode (SCE) was taken as reference electrode and platinum as a counter electrode. The following equations was used to evaluate the protection efficiency of the coating.

$$P(\%) = \frac{R_{ct} - R_{ct}^*}{R_{ct}} \times 100 \quad (1)$$

$$P(\%) = \frac{i_{corr}^* - i_{corr}}{i_{corr}^*} \times 100 \quad (2)$$

Where, P(%) is the protection efficiency, R_{ct} and R_{ct}* is the charge transfer resistance of coated and uncoated substrate, i_{corr} and i_{corr}* is the corrosion current density coated and uncoated substrate.

2.4.2 Weight loss method

To further evaluate corrosion properties of as-prepared PANI/SiO₂ coated mild steel was extensively studied by weight loss method. The bare and PANI/SiO₂ coated mild steel with a dimension of 2cm×3cm were immersed in 1.0 mol L⁻¹NaCl medium for 30 days. Before and after immersion, the bare and coated mild steel were weighed in the electronic balance. After 30 days, the test specimens were removed from the solution and washed exhaustively with distilled water, followed by acetone and dried in air. The changes in the coated substrate were visually inspected after 30 days of immersion. Moreover, the changes in weight were calculated according to the weight loss (g cm⁻² h⁻¹) formula as follows

$$W_L = \frac{W_1 - W_2}{at} \quad (3)$$

The corrosion rate (CR) of the PS coated mild steel substrate was estimated by weight loss method using the following equation.

$$CR(mm\text{year}^{-1}) = \frac{(W_1 - W_2) \times 87.6}{atd} \quad (4)$$

Where, W_1 is the initial weight (before immersion) of the sample (mg), W_2 final weight (after immersion) of the sample (mg), a is the surface area of the sample (cm^2), t is the end time of immersion (h) and d is the density of bare mild steel substrate (7.85 g cm^{-3}).

3. Results & Discussion

3.1 FTIR analysis

Fig 1. Represents the FTIR spectra of PANI Neat and PANI/SiO₂ nanocomposites, respectively. The peak corresponding to 1575 and 1483 cm^{-1} represented the stretching vibration of C=N and C=C in all the samples. The bands at 1292 cm^{-1} and 1245 cm^{-1} confirmed the C–N stretching mode of the benzenoid ring. The peak at 1118–1112 cm^{-1} assigned to C–H mode in plane bending vibration during protonation [21]. The FTIR spectrum corresponding to the presence of SiO₂ was observed at 1061 cm^{-1} and 807 cm^{-1} attributed to the stretching and bending vibrations of Si–O–Si, respectively. The C–N stretching vibration in protonic acid doped PANI from PANI-SDBS, where SO_3^- group of SDBS is bounded with the nitrogen atom of PANI was observed at 1302 cm^{-1} . Further in the case of PSC there was shift of peaks to higher wavenumbers at 1565 cm^{-1} , 1483 cm^{-1} , 1292 cm^{-1} and 1245 cm^{-1} respectively as compared with neat PANI due to the dispersion of silica nanoparticles in the matrix. Similarly, the bending vibration of Si–O–Si peak at 1056 cm^{-1} was found to be shifted to lower wavenumbers. The behaviours indicated interaction between PANI and SiO₂ nanoparticles.

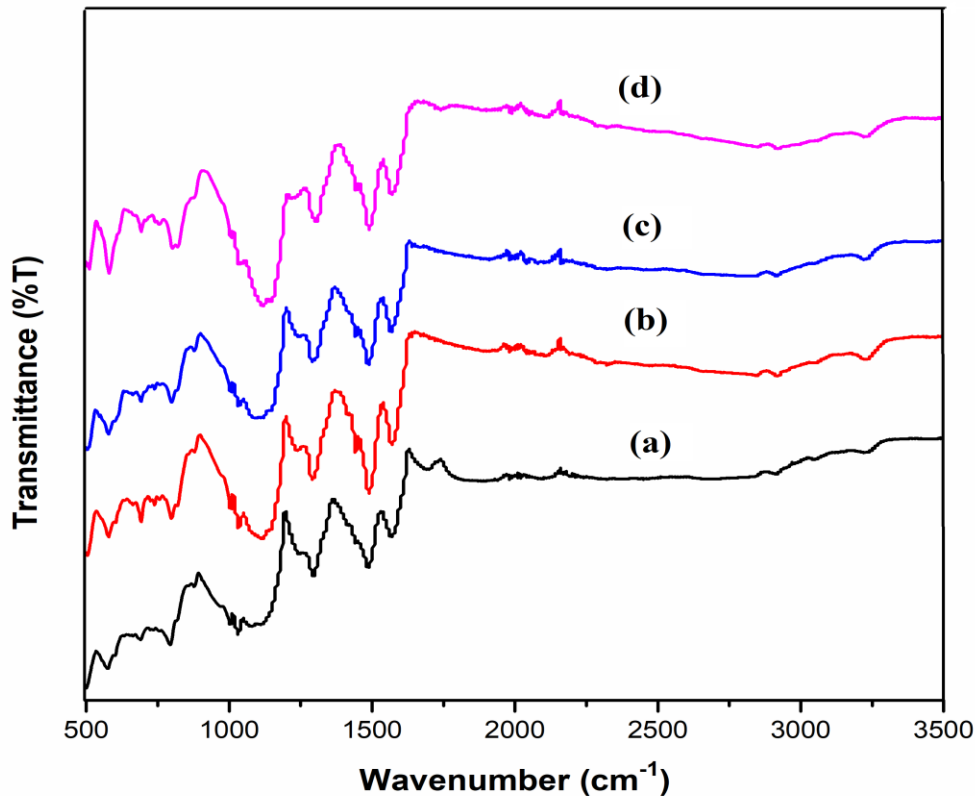


Fig 1. FT-IR spectra of (a) PANI neat, (b)PSC-I, (c)PSC-II, and (d)PSC-III

3.2XRD analysis

The XRD pattern of PANI and PANI/ SiO₂ is represented in Fig 2. The peak related to PANI was observed at $2\theta = 20$ and 25° , indicating (020) (200) semi-crystalline planes as reported by Chin et al. [22]. However, with the incorporation of SDBS, the intensity of the d200 peak reduced in presence of dopant. Further as observed from the x-ray diffractograms of PANI/SiO₂ nanocomposite it is observed that a relatively intense peak at $2\theta = 20$ was observed which revealed higher crystalline nature of PANI in presence of the dopant and SiO₂.

On contrary, Chei et al. [22], had reported in their work that SiO₂ has no influence on the crystallinity of PANI. Hence, it can be concluded that addition of SiO₂ has considerable effect on PANI and that might be due to the absorption of PANI on SiO₂ surface in presence of SDBS [23].

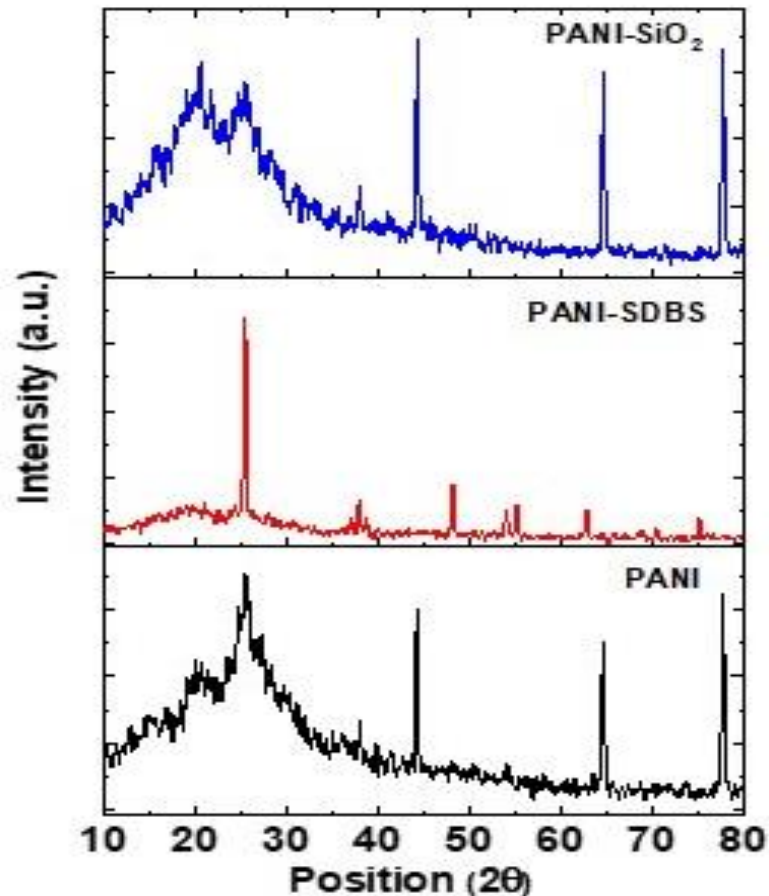


Fig.2. XRD pattern of neat PANI , PANI-SDBS and its nano composites

3.3 TEM Studies

Fig 3 shows the TEM image of PANI/ SiO₂ composites. From the figure, it is clear that the SiO₂ nanoparticles are uniformly distributed in the PANI matrix. This uniform distribution of SiO₂ in the composite may be due to the incorporation of SDBS that acts as dispersant and might be held responsible for the control of homogeneity in the composite. The agglomerated structure of PSC also found due to interparticle interaction of SiO₂. Further, a portion of the micrograph has been found to be dark indicating the thickness of the sample was too high for TEM imaging due to mass contrast phenomena.

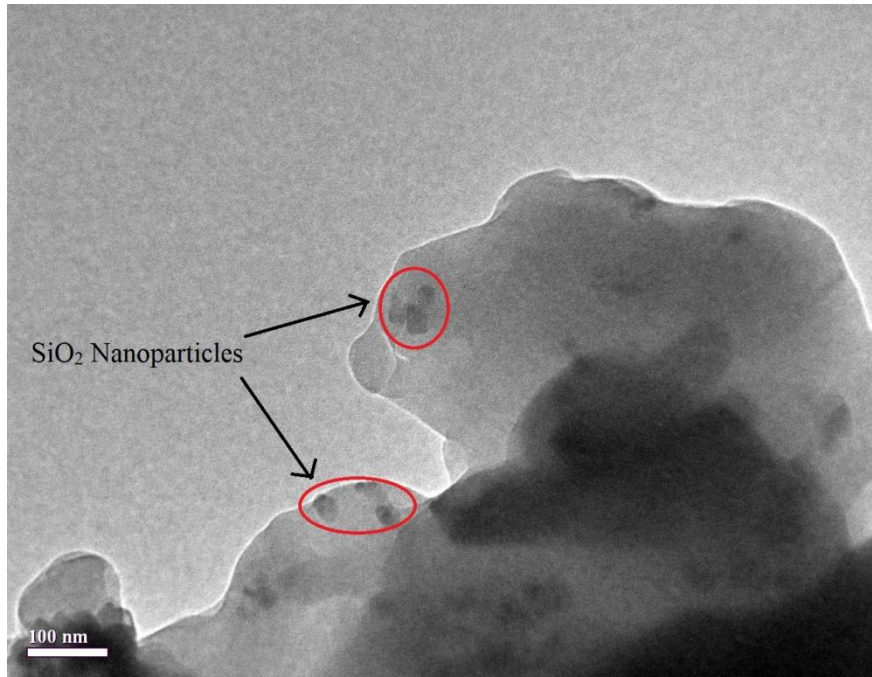


Fig 3. TEM image of PANI/ SiO2 composites

3.4 AFM studies

The surface morphology of PANI neat and PSC thin films were characterized by Atomic Force Microscopy technique. Figures 4 (a) and (b) shows the 3D Atomic Force Microscopic images of PANI neat and PSC respectively. .

As observed from the AFM micrographs the SiO₂ nanoparticles were dispersed uniformly within the PANI matrix. Also it may be noted that the nanocomposites sample displayed increasing root-mean-square (RMS) surface roughness value of 16.06 nm as compared with neat PANI which had an RMS value of 5.87.

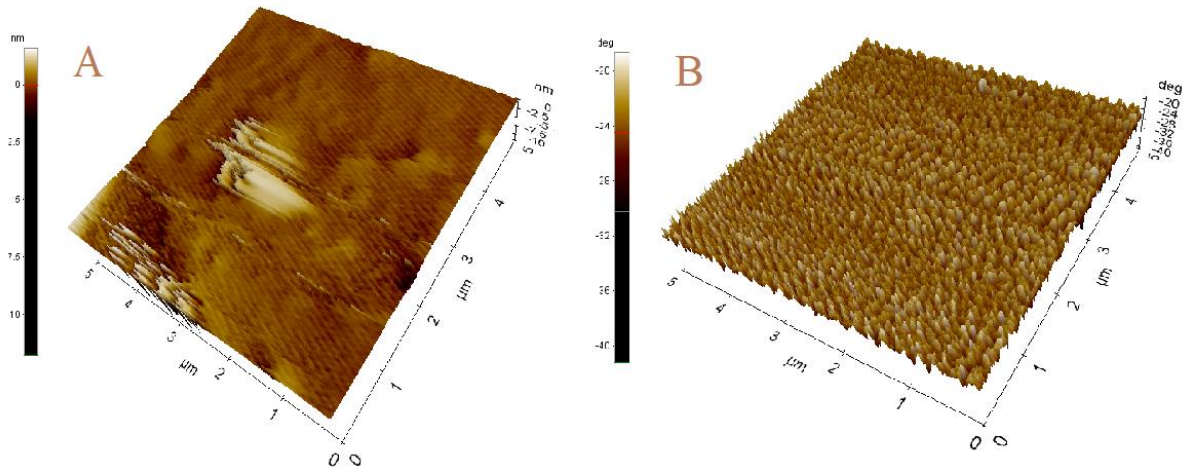


Fig 4. 3D Atomic Force Microscopic images of (a) PANI neat and (b) PANI/SiO₂-III

3.5 Contact angle

This wettability characteristics of the coated surfaces was tested using contact angle measurements. The data of water contact angle measurements showed that the surface paint had shown fig 5. The hydrophilic nature because the contact angle is less than 90 degree. The measurements revealed that the surface contact angle of PANI Neat and PANI/SiO₂-III nanocomposite was found to be 64° and 73°, respectively as shown in Fig.5. This shows an improvement of the PANI/SiO₂ in the wettability characteristics as compared to the neat counterpart. Therefore the results indicate that the incorporation of SiO₂ reduces the hydrophilicity.

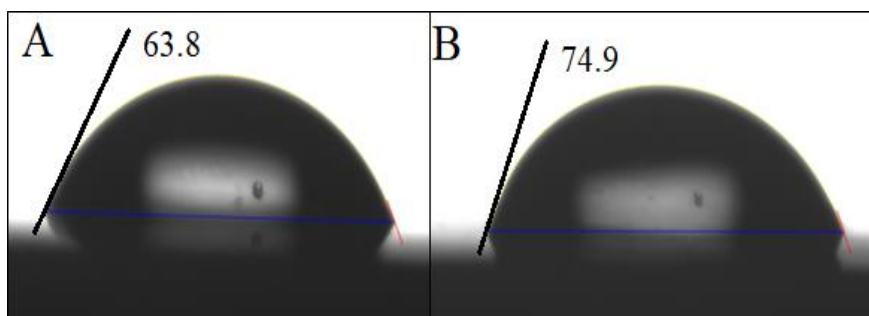


Fig 5. Contact angle of (A) PANI Neat, (B) PANI/SiO₂ composite

3.6 TGA Studies

TGA thermograms of PANI Neat, and PANI/ SiO₂-III nanocomposites are depicted in Fig. 6. As observed from the thermograms PANI Neat displayed (Fig.6) a three decomposition. The initial decomposition observed at 240⁰C with a corresponding weight loss of about 3–10 % may be attributed to the loss of residual water trapped in the PANI matrix and other volatiles. The decomposition in the second stage at 310 to 450 ⁰C involves the loss of dopant SDBS as well as the initial degradation of the backbone the matrix polymer. The third stage decomposition observed beyond 570⁰C indicated the degradation of both SDBS and PANI. SiO₂ nanoparticles have thermal stability up to 800⁰C. Thus, incorporation of SiO₂ within the PANI matrix improved the thermal stability which is predominantly due to the barrier layer formed by the nanoparticles that prevent outflow of the decomposition of products [24].

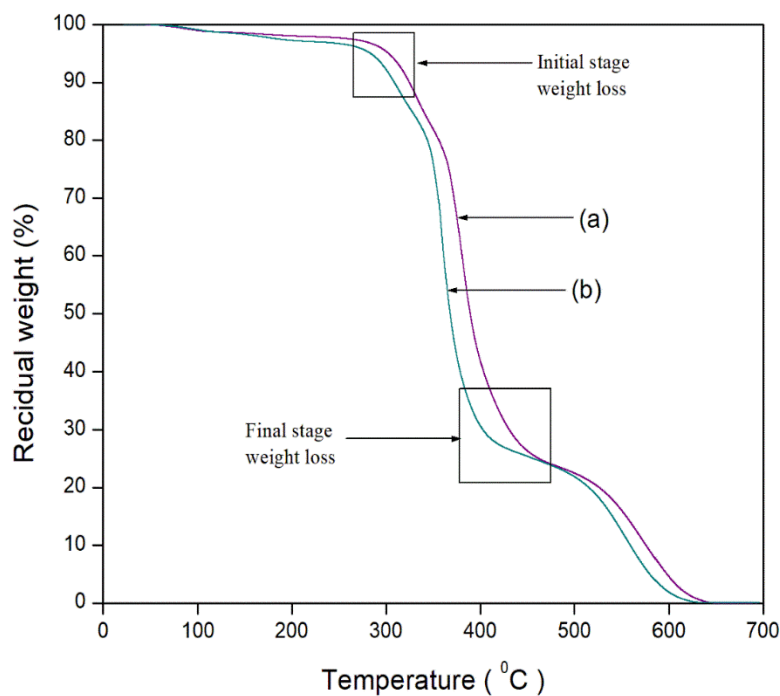


Fig 6. TGA Curves of (a) PANI Neat, (b) PANI/SiO₂ composite

3.7 Corrosion studies (weight loss method)

Table 1. Weight loss parameter during the immersion test in 3.5% NaCl for 30 days

Sample name	Initial weight (mg)	Weight after immersion 3.5%NaCl for 30 days	Weight loss (mg)	Weight loss (%)	Corrosion rate (mm/year)
Blank Mild Steel	4283.1	3669.76	613.34	14.32	1.59
Epoxy (Blank)	4783.6	4227.26	556.34	11.63	1.44
PANI neat	4967.5	496.58	470.92	9.48	1.21
PANI/SiO ₂ -I	4872.8	4456.66	416.14	8.54	1.08
PANI/SiO ₂ II	4678.3	4373.28	305.02	6.52	0.79
PANI/SiO ₂ III	4769.1	4531.60	237.50	4.98	0.61

The corrosion rates(CR) in mm/year of blank mild steel, epoxy blank, PANI Neat and PANI/SiO₂ is represented in Table 1. As observed from the table the weight loss % in blank mild steel was 14.32 % which reduced to 11.63% after coating with epoxy. Further in case of PANI coated samples the weight loss was 9.38% in 3.5% NaCL after 30 days time period.

However, the PANI/SiO₂ coated panels showed improved performance in which the weight loss was 4.98%. Comparing the CR rates, it is evident from the test results reported in Table 1, after 30 days of immersion of the blank mild steel, the CR value was 1.59/year which reduced drastically to 0.61 mm/year approximately to the tune of 160% thus revealing the efficacy of the coated nanocomposite panels [21].

Electrochemical studies of PS/MS Coatings

The corrosion properties of as-prepared coatings were analyzed by EIS and Tafel techniques in 3.5% NaCl solution. The Tafel curves acquired for the mild steel, epoxy coating and PANI-SiO₂ epoxy coating were shown in **Fig 7**. The corrosion potential and current density of the blank and coated substrates were obtained from the Tafel curves by the intersection of the extrapolation of anodic and cathodic curves. The calculated electrochemical parameters were given in the **Table 2**. It is observed that the PS/MS coatings showed improved corrosion resistance compared to the epoxy coatings and bare substrate by decreasing the corrosion current density (I_{corr}) and the shift toward the positive side in corrosion potential (E_{corr}). Moreover, the PS/MS coatings revealed higher protecting efficiency of 90% compared to other coatings and substrates.

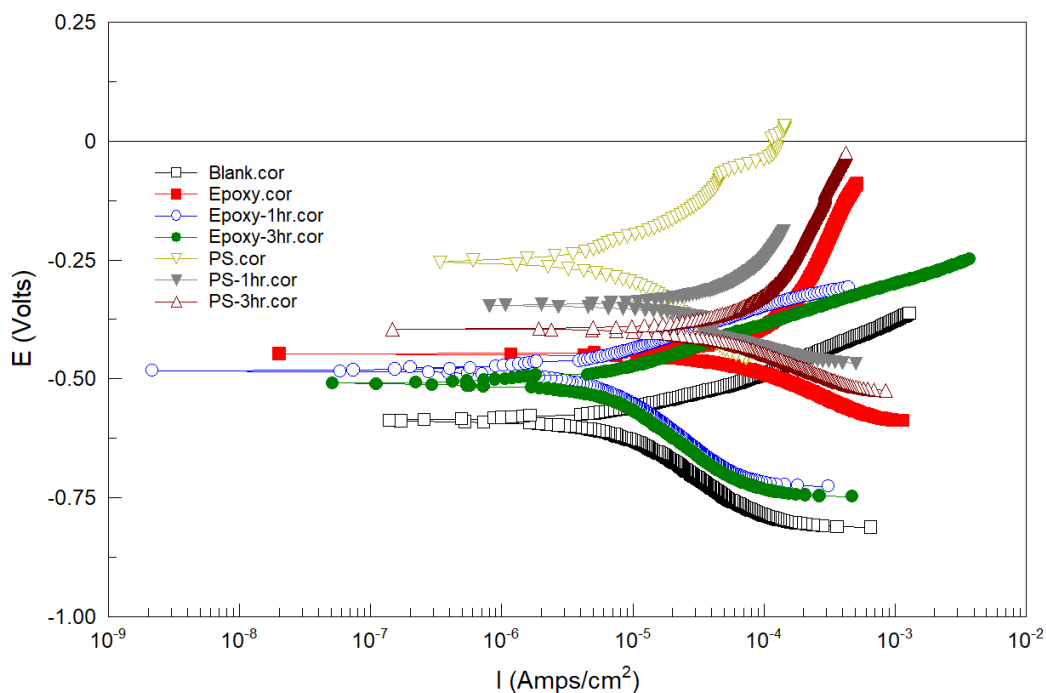


Figure. 7 Electrochemical properties of mild steel, epoxy and PS coatings.

The charge transfers resistance and capacitance of the blank and as-prepared coatings were tested by electrochemical impedance spectroscopy. The bode profiles of the mild steel, epoxy coating and PANI-SiO₂ epoxy coatings were displayed in **Fig 8**. From the curve, it is observed that the increase in charge transfer resistance and decrease in capacitance indicates the better corrosion resistance property of as-prepared PS/MS coatings over epoxy and bare substrate. Moreover, from the periodic evolution, the PS coatings provide better corrosion-resistant performance than epoxy coating. However, a decrease in performance when increasing the immersion time it might be due to the slightly porous nature of the coating induces the corrosion phenomena. The results demonstrate that the PS coating itself has a barrier and redox property, which improves corrosion protection performance.

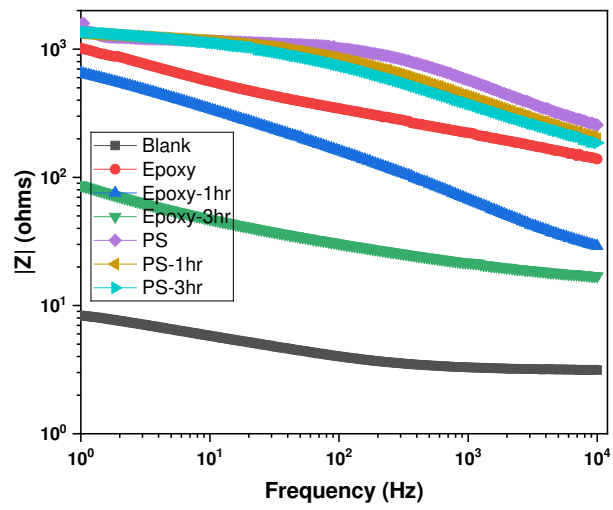


Figure 8. Bode plots of mild steel, epoxy and PS coatings.

Table:2 Protection performance of PS and Epoxy coatings on steel in 3.5 % NaCl

Samples	EIS			Tafel		
	R_{ct} $\Omega \text{ cm}^2$	C_{dl} $\mu\text{F}/\text{cm}^2$	Protection Efficiency (%)	I_{corr} $\mu\text{A}/\text{cm}^2$	E_{corr} mV vs SCE	Protection Efficiency (%)
Blank	4.9	32	--	564	-588	--
Epoxy0 hr	547	22	99	92	-447	83
Epoxy 1 hr	141	11	96	80	-482	85
Epoxy 3 hr	91	18	94	82	-505	85
PS 0 hr	1262	707	99	54	-253	90
PS 1 hr	1191	161	99	93	-364	82
PS 3 hr	470	369	98	78	-395	86

4. CONCLUSION

PANI / SiO₂nanocomposites have been successfully prepared by situ solution polymerization in aqueous solution containing SDBS as a dopant with different weight ratios of SiO₂/aniline. The synthesis and curing of the composites were confirmed by spectral studies. Contact angle analysis indicate the increase in contact angle value due to the incorporation of SiO₂. TGA results revealed that inclusion of SiO₂ nanoparticles improves the thermal stability of composite to a smaller extent due to the interaction of SiO₂ particles and PANI matrix. TEM images of nanocomposites showed the polymer growth on the surface of SiO₂ particles. AFM studies indicate the surface roughness value can be increasing by incorporation SiO₂ nanocomposites. Corrosion study shows that PANI and PANI/SiO₂nanocomposites coating show good corrosion resistance property on mild steel in 3.5 % NaCl aqueous solution. The results also revealed that corrosion protection property depends on SiO₂ content in composite coating and better corrosion resistance is observed for the formulation containing 0.20SiO₂ (PSCIII).

References

1. A. Stierle, Tracking corrosion cracking. Science 321, 349–350 (2008)
2. F U. Renner, et al. Initial corrosion observed on the atomic scale. Nature 439, 707–710 (2006)
3. Q. Wang, B.W. Zhang, M.N. Qu, J.Y. Zhang, D.Y. He. Appl. Surf. Sci. 2008; 254: 2009
4. JC. Lacroix, JL. Camalet, S. Aeiych, KI. Chane-Ching, J. Petitjean, E.Chauveau, Electroanal. Chem 2000; 481:76.
5. AG.Mac Diarmid, J C.Chiang, and A F.Richter, Synth Met 18 (1987) 28
6. A K.Bakhshi, and G J .Bhalla, Sci Ind Res 63-715 (2004)
7. G M Spinks, A J Dominis, G G Wallace, and D E Tallman, Solid State Electrochem 6 - 85 (2002).

8. M Angelopoulos, IBM J RES & DEV 45-57 (2001).
9. P K Khanna, M V Kulkarni, N Singh, S P Lonkar, V V V V S Subharao, and A K Visvanath, Mater ChemPhys 95 (2006).
10. G Majumdar, M Goswami, TK Sarma, A Paul, and A Chattopadhyay, Langmuir 21:1663(2005).
11. D Chowdhury, A Paul, and A Chattopadhyay, Langmuir 21:4123(2005).
12. XM Feng, G Yang, WH Hou, and Zhu JJ, Macromol Rapid Commun 27:31(2006).
13. Al-Dulaimi, and S Hashim, Int. J. Mech. Mater. Eng. 7 113 (2012)
14. M Hasan, Y Zhou, S Mahfuz and S Jeelani, Mater Sci Eng A 429: 181 (2006)
15. Li X, Dai, G Wang and X Song Appl Polym Sci 107:403 (2008)
16. HS Xia, and Q Wang, Appl Polym Sci 87:1811 (2003).
15. H Zengina, and B Erkan, Polym Adv Technol 21:216 (2010)
18. H Bhandari, V Choudhary, and SK Dhawan, Thin Solid Films, 519: 1031 (2010)
19. J Iribarren, E Armelin, F Liesa, J Casanovas, and CAleman 57: 683 (2006).
20. KS Rao, KEI-Hami, T Kodaki, K Matsushige and K Makino, J Colloid Interface Sci 289:125(2005)
21. S. Hema Bhandari, S. Anoop Kumar and, K. Dhawan Chapter <http://dx.doi.org/10.5772/50470>, 2012
22. S. Y. Chin, T. K. Abdullah, · M. Mariatti, J Mater Sci: Mater Electron (2017)
23. R C Rathod, V K Didolkar, S S Umare, and B H Shambharkar, Trans Indian Inst Met 43-64 (2011)
24. M Rohwerder, L Duc, A Michalik, Coatings. Electrochem. Acta 54, 6075–6081 (2009)

Figures

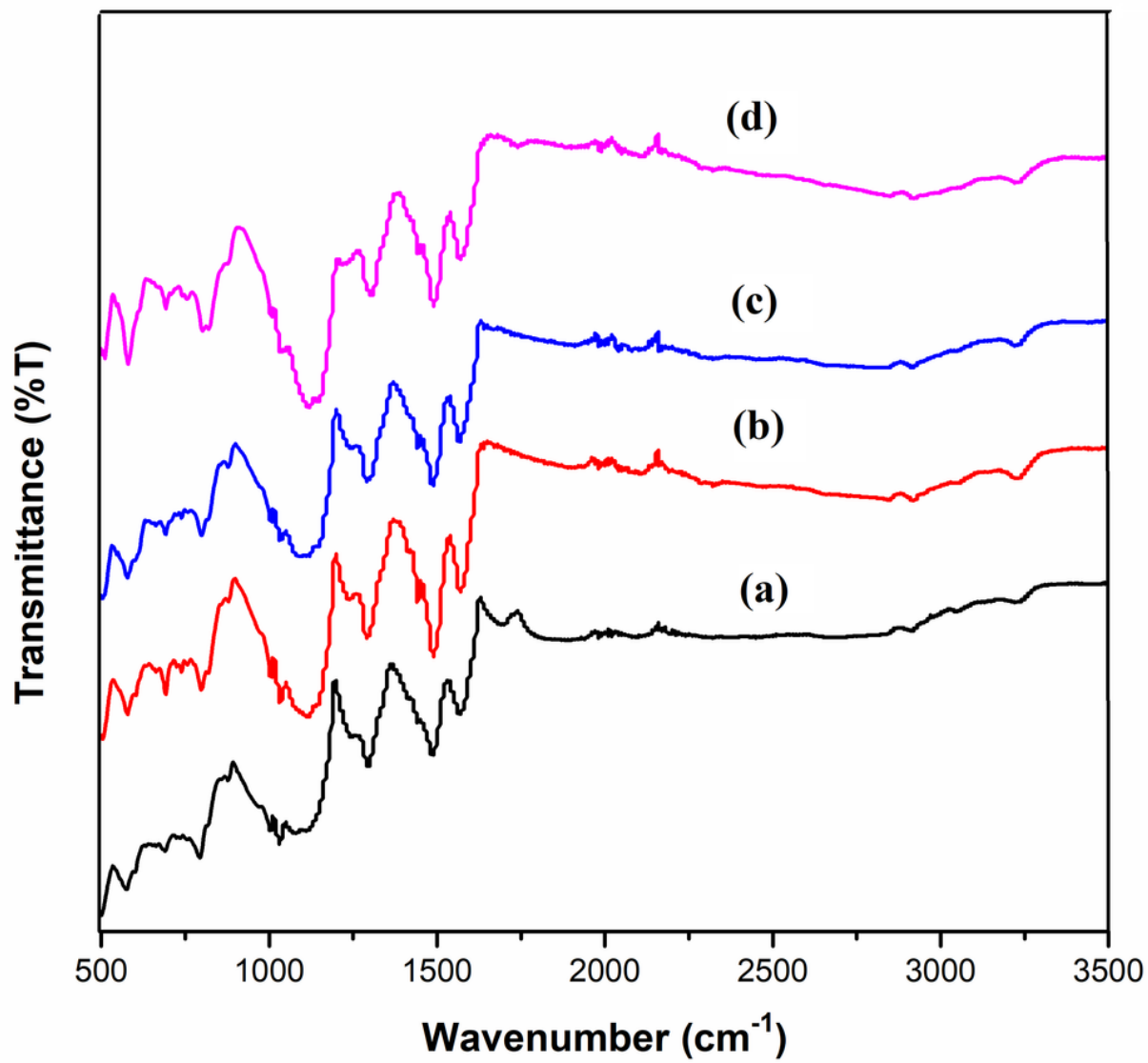


Figure 1

FT-IR spectra of (a) PANI neat, (b)PSC-I, (c)PSC-II, and (d)PSC-III

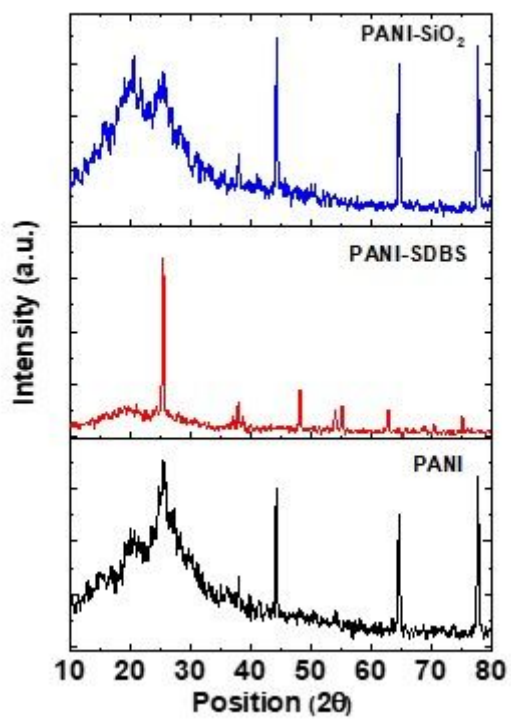


Figure 2

XRD pattern of neat PANI , PANI-SDBS and its nano composites

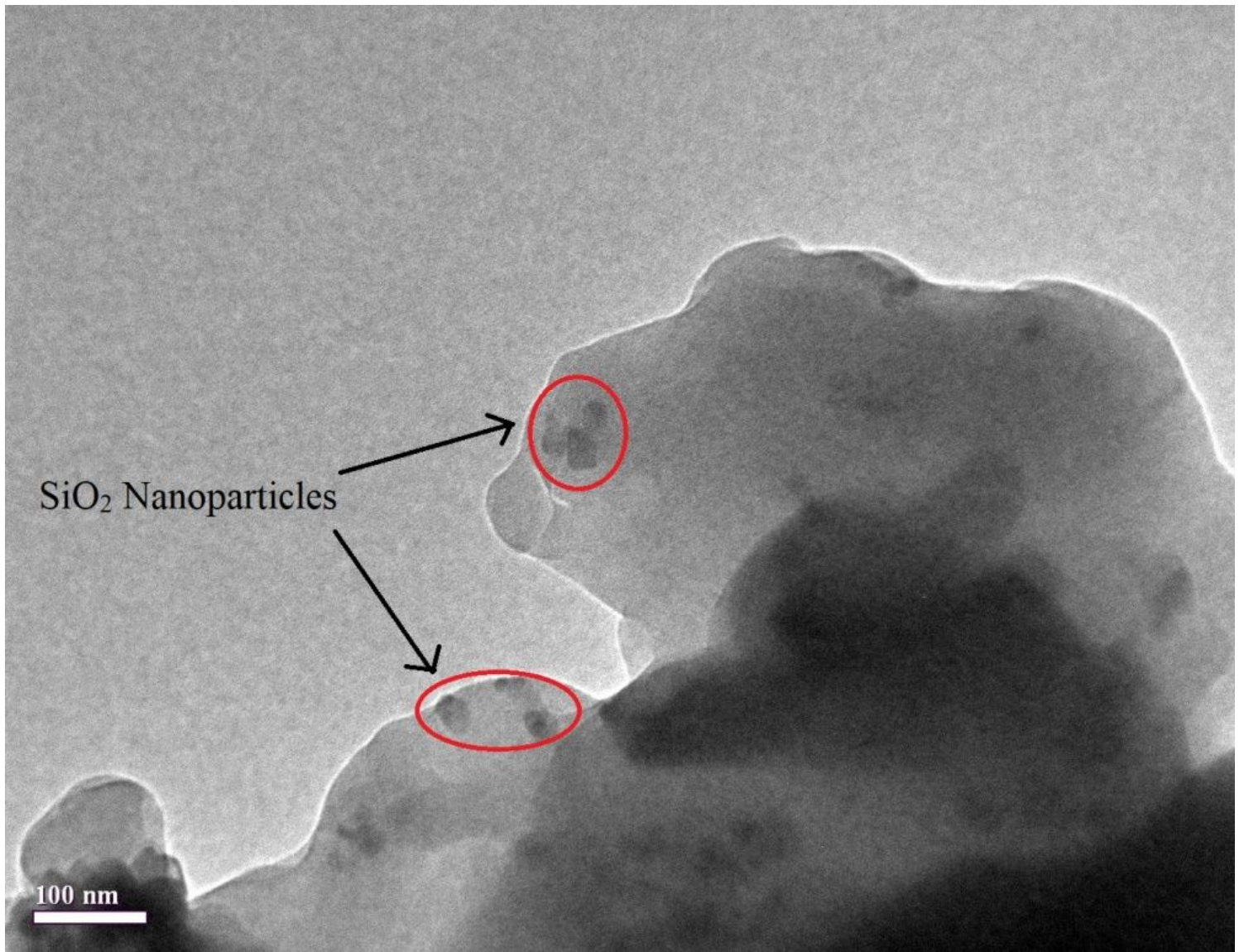


Figure 3

TEM image of PANI/ SiO₂ composites

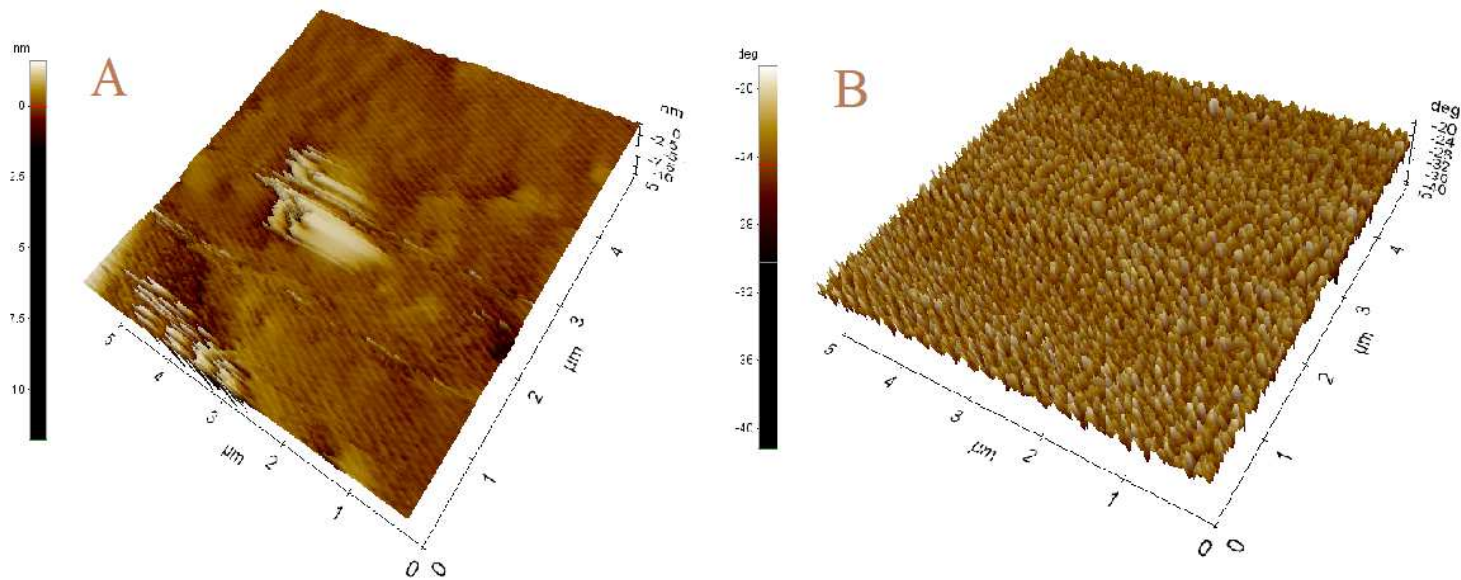


Figure 4

3D Atomic Force Microscopic images of (a) PANI neat and (b) PANI/SiO₂-III

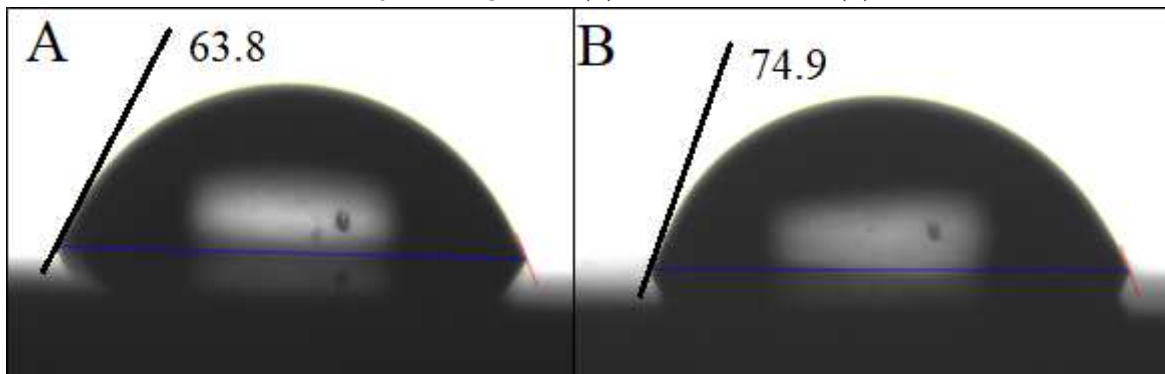


Figure 5

Contact angle of (A) PANI Neat, (B) PANI/SiO₂ composite

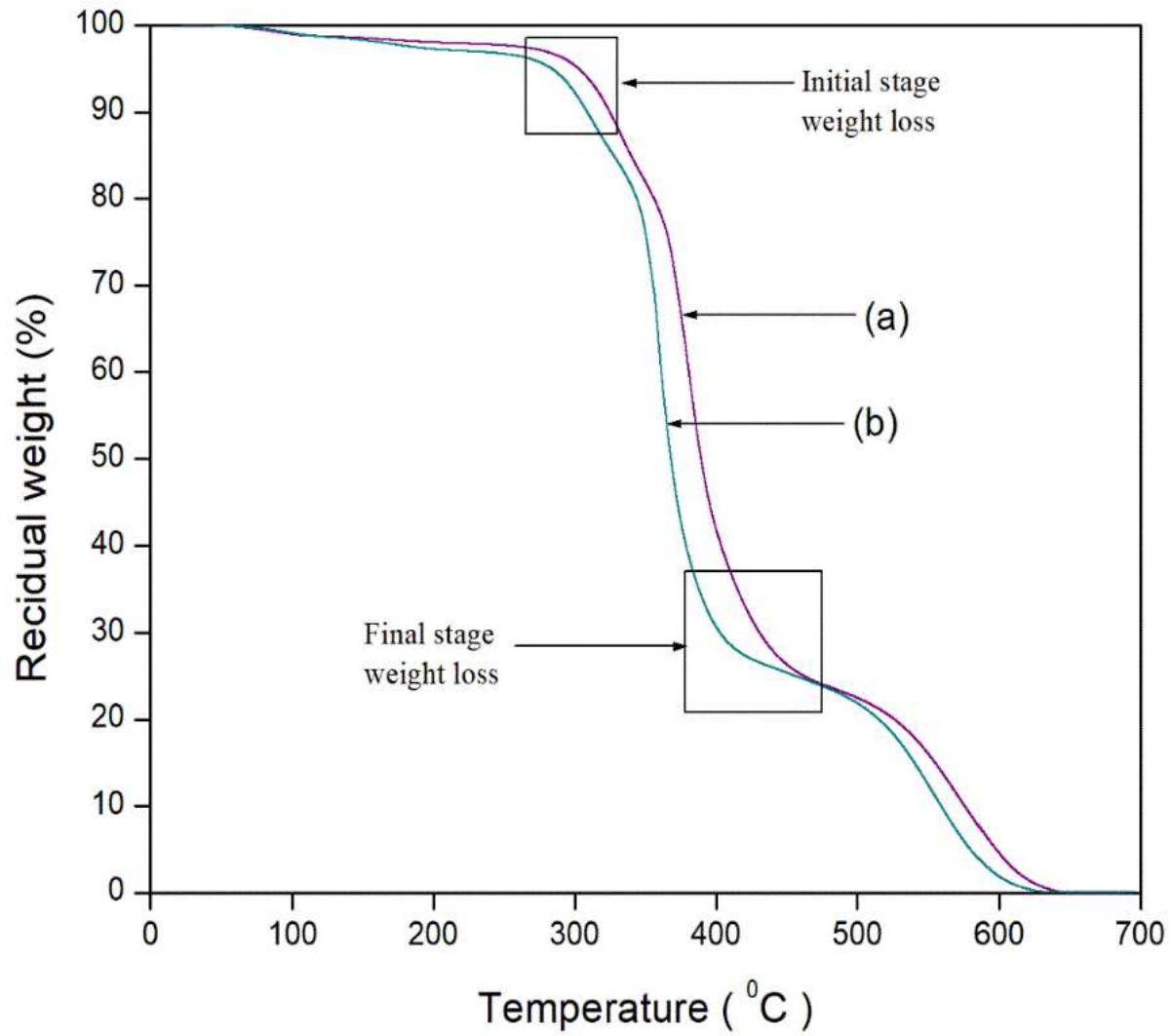


Figure 6

TGA Curves of (a) PANI Neat, (b) PANI/SiO₂ composite

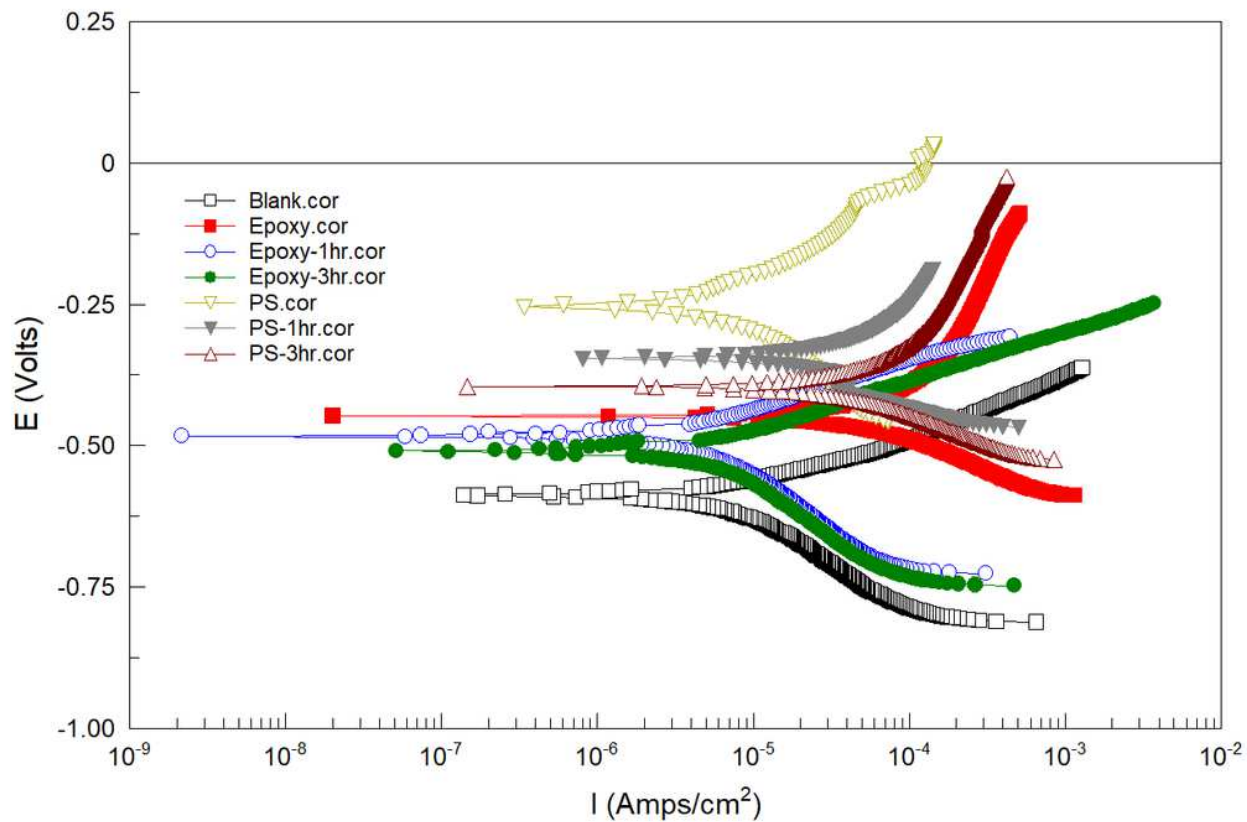


Figure 7

Electrochemical properties of mild steel, epoxy and PS coatings.

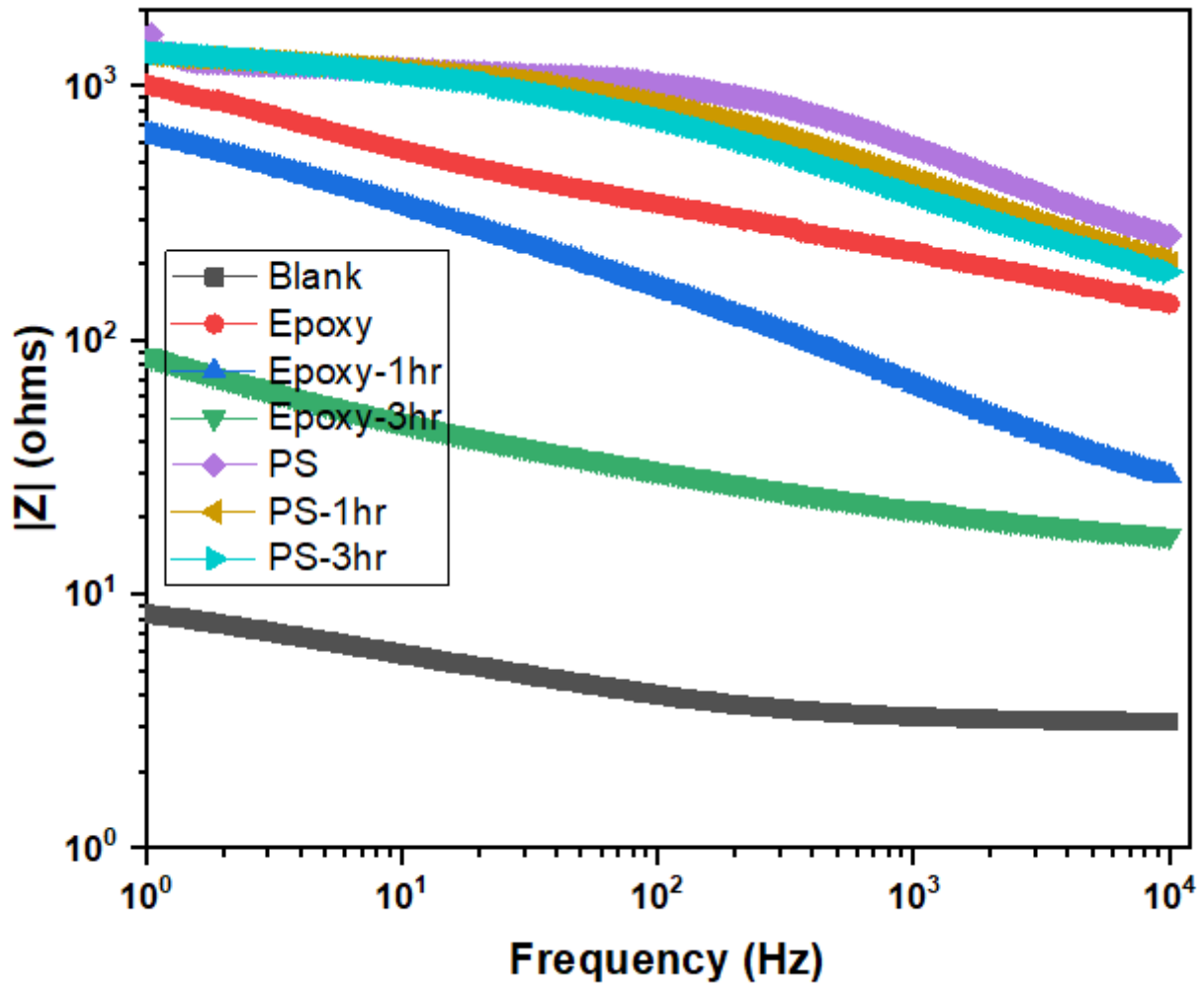


Figure 8

Bode plots of mild steel, epoxy and PS coatings.